Drug Delivery

DOI: 10.1002/ange.201406216

Cell-Mediated Assembly of Phototherapeutics**

*Weston J. Smith, Nathan P. Oien, Robert M. Hughes, Christina M. Marvin, Zachary L. Rodgers, Junghyun Lee, and David S. Lawrence**

Abstract: *Light-activatable drugs offer the promise of controlled release with exquisite temporal and spatial resolution. However, light-sensitive prodrugs are typically converted to their active forms using short-wavelength irradiation, which displays poor tissue penetrance. We report herein erythrocyte-mediated assembly of long-wavelength-sensitive phototherapeutics. The activating wavelength of the constructs is readily preassigned by using fluorophores with the desired excitation wavelength λ_{ex}. Drug release from the erythrocyte carrier was confirmed by standard analytical tools and by the expected biological consequences of the liberated drugs in cell culture: methotrexate, binding to intracellular dihydrofolate reductase; colchicine, inhibition of microtubule polymerization; dexamethasone, induced nuclear migration of the glucocorticoid receptor.*

The use of light to activate therapeutic agents at disease sites offers the advantage of aggressive treatment with exquisite spatial control, thereby reducing potential deleterious side effects at unintended sites. An excellent example of this concept is photodynamic therapy, which employs the delivery of a photosensitizer to the tissue of interest.[1] Upon excitation with the appropriate wavelength of light and, in the presence of oxygen, cytotoxic reactive oxygen species are generated, resulting in destruction of the target cells. This minimally invasive procedure furnishes control over where and when the reactive oxygen species are produced. However, a more general strategy that can control the delivery of any drug could profoundly influence the treatment of a variety of disorders, including cancer, diabetes, and autoimmune and vascular diseases. A major challenge in this regard is the so-called "optical window of tissue", the wavelength of light with maximal tissue penetration, which lies in the range of 600–900 nm.[2] Wavelengths less than 600 nm are absorbed by hemoglobin in the circulatory system and melanin in the skin, whereas water interferes with light penetration for wavelengths greater than 900 nm. Unfortunately, nearly all light-activatable prodrugs described to date respond to short-wavelength irradiation < 450 nm.[3] This limitation is responsible for the intense interest in two-photon[4] and up-converting[5] technologies. However, as discussed in recent reviews,[4,5] both technologies must overcome daunting challenges before potential therapeutic applications are realized. We recently described the long-wavelength (> 600 nm) photolysis of alkylcobalamins (alkyl-Cbl).[6] We now report the cell-mediated assembly of lipid-Cbl-drug and lipid-fluorophore conjugates in which the latter serve as long-wavelength-capturing antennas that promote drug release.

Erythrocytes have been called the "champions of drug delivery" due to their biocompatibility, their long lifespan (120 days), and their size, which allows large quantities of drug to be conveyed relative to other carriers.[7] However, "practically useful controlled release from carrier RBC (red blood cells) remains an elusive goal".[7] Our strategy to address this issue is depicted in Figure 1. Based on a previously demonstrated energy transfer between fluorophores and Cbls in covalently appended Cbl-fluorophore conjugates,[6] we decided to explore the premise that the cell-mediated assembly of C_{18}-Cbl-drug and C_{18}-fluorophore conjugates could act in concert as a photoresponsive drug-delivery system. Illumination of the fluorophore antenna at its λ_{max} and subsequent energy transfer to the Cbl-drug moiety should result in cleavage of the weak Co–C bond,[6,8] thereby liberating the drug.

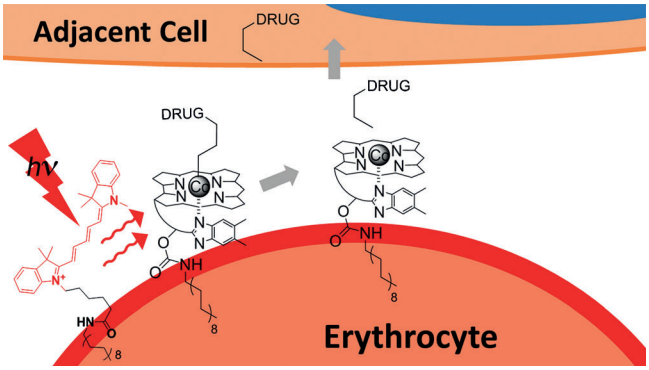

Figure 1. A wavelength-encoded drug-release strategy. Anti-inflammatory drugs are covalently appended to Cbl by means of a photolabile Co–C bond. Lipidated-Cbl and fluorophore constructs assemble on the plasma membrane of human erythrocytes. The fluorophore serves as an antenna, capturing long-wavelength light and transmitting the energy to the Cbl-drug conjugate, resulting in drug release from the erythrocyte carrier.

A series of lipidated Cbl (C_{18}-Cbl) and C_{18}-fluorophore derivatives were prepared (Figure 2; Figures S1–S4, Tables S3–S6, and Scheme S1 in the Supporting Information (SI)). In the case of the Cbl derivatives, the C_{18} moiety was

[*] W. J. Smith, N. P. Oien, Dr. R. M. Hughes, C. M. Marvin, Z. L. Rodgers, J. Lee, Prof. D. S. Lawrence
Department of Chemistry, Division of Chemical Biology and Medicinal Chemistry, and Department of Pharmacology
University of North Carolina, Chapel Hill, NC 27599 (USA)
E-mail: lawrencd@email.unc.edu

[**] We thank the NIH for financial support (R01 CA79954) and Prof. Melanie Priestman for assistance with the imaging experiment in the Supporting Information, Figure S8.

Supporting information for this article is available on the WWW under http://dx.doi.org/10.1002/anie.201406216.

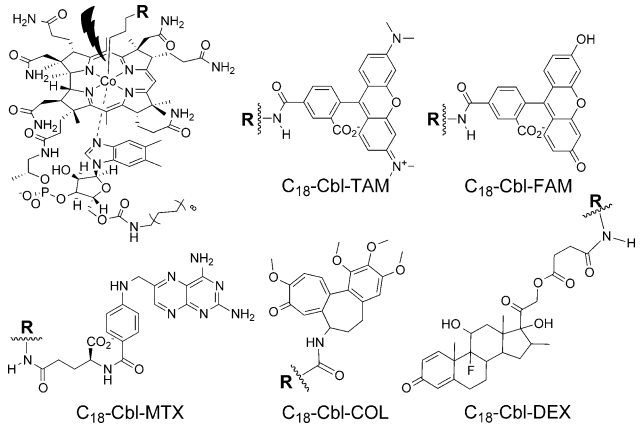

Figure 2. Anti-inflammatory drugs are lipidated Cbl-reporters, TAM (C_{18}-Cbl-TAM) and FAM (C_{18}-Cbl-FAM) and lipidated Cbl-drug conjugates, MTX (C_{18}-Cbl-MTX), COL (C_{18}-Cbl-COL), and DEX (C_{18}-Cbl-DEX).

appended to the 5′ ribose hydroxy group of Cbl using octadecylamine and carbonylditriazole. Subsequent alkylation of the Co furnished an amine or carboxylic acid handle, to which drugs and fluorescent reporters were covalently attached (Figure 2; Figure S5 and Schemes S2–S7 (SI)). These species include the anti-inflammatories methotrexate (MTX), colchicine (COL), and dexamethasone (DEX), and the fluorescent reporters tetramethylrhodamine (TAM) and fluorescein (FAM). The C_{18}-fluorophore derivatives were prepared by direct condensation of the activated carboxylate of the fluorophore with the amine of octadecylamine (Schemes S8–S10 (SI)).

Our initial studies sought to explore the premise of the strategy outlined in Figure 1 by establishing the light-triggered movement of drugs and reporters from a hydrophobic environment to an aqueous one. For these preliminary experiments we directly photolyzed C_{18}-Cbl-drug and C_{18}-Cbl-reporter conjugates at the Cbl absorbance wavelength (525 nm). As expected, both C_{18}-Cbl-TAM and C_{18}-Cbl-MTX are soluble in octanol. Illumination at 525 nm cleaved the Co–C bond in C_{18}-Cbl-TAM and promoted migration of TAM from octanol to water as assessed by fluorescence (Figure S6 (SI)). In an analogous fashion, 525 nm illumination of C_{18}-Cbl-MTX triggered the release of MTX into the aqueous phase as demonstrated by LC-MS (Figure S7 (SI)). We subsequently explored the light-triggered transfer of drug/reporter from the lipophilic plasma membrane of erythrocytes to the aqueous milieu. First, exposure of erythrocytes to C_{18}-Cbl-TAM furnished even and extensive loading as assessed by widefield fluorescence microscopy. In addition, given the established photolytic sensitivity of the Co–C bond,[6,8,9] we were not surprised to find that imaging C_{18}-Cbl-TAM on erythrocytes results in the rapid migration (<1 s) of TAM fluorescence from erythrocytes into solution (Figure S8 (SI)).

C_{18}-Cbl-MTX, C_{18}-Cbl-COL, and C_{18}-Cbl-DEX were loaded onto intact human erythrocytes with minimal lysis (ca. 5% at 5 μM C_{18}-Cbl-drug, Figure S9 (SI)). The amount of C_{18}-Cbl-drug loaded per red blood cell was 0.3–1.0 fmol. Subsequent photorelease of the drug was quantitative for C_{18}-Cbl-COL and C_{18}-Cbl-DEX and 35% for C_{18}-Cbl-MTX (Figure S10 (SI)):

C_{18}-Cbl-MTX: LC-MS analysis revealed that photolysis of erythrocyte-anchored C_{18}-Cbl-MTX primarily furnishes *N*-propylamide MTX (Figure 3; Scheme 11 and Tables S4–S6

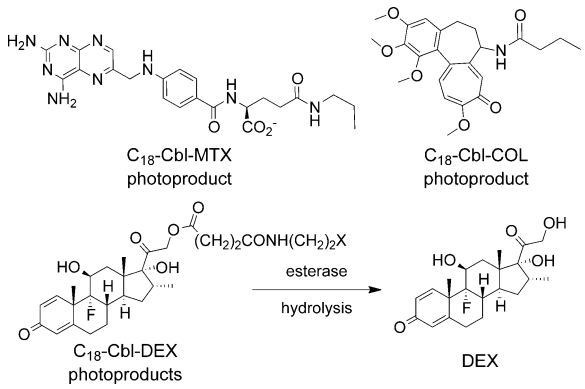

Figure 3. Erythrocyte-released photoproducts of C_{18}-Cbl-MTX, C_{18}-Cbl-COL, and C_{18}-Cbl-DEX. In the case of C_{18}-Cbl-DEX, DEX is observed, instead of the possible photoproducts (X = H, OH, or = O).

(SI)). Consistent with the established structure–activity relationship of MTX derivatives,[10] the photolyzed product of C_{18}-Cbl-MTX serves as an effective inhibitor of dihydrofolate reductase (DHFR, Figure S11 (SI)). In addition, photoreleased MTX from erythrocyte-anchored C_{18}-Cbl-MTX binds to DHFR in HeLa cells (Figure S12 (SI)).

C_{18}-Cbl-COL: *N*-butanoyl COL is the primary photoproduct of C_{18}-Cbl-COL-loaded erythrocytes (Figure 3; Tables S4–S6 (SI)). Photolyzed C_{18}-Cbl-COL disrupts microtubules in HeLa cells as effectively as COL itself (Figures S13 and S14 (SI)).

C_{18}-Cbl-DEX: DEX is the observed product from photolysis of C_{18}-Cbl-DEX-loaded erythrocytes, instead of one or more of the expected photoproducts (Figure 3; Tables S4–S6 (SI)). The 21-esters of DEX are prodrugs that are hydrolyzed to DEX in vivo.[11] The possible presence of blood esterases[12] may explain the formation of DEX once the conjugate is freed from the RBC surface. Photorelease of DEX from C_{18}-Cbl-DEX-loaded erythrocytes cocultured with HeLa cells results in the migration of glucocorticoid receptor α (GRα) from the cytosol to the nucleus in HeLa cells (Figures S15 and S16 (SI). We note that, in the absence of illumination, C_{18}-Cbl-MTX-, C_{18}-Cbl-COL-, and C_{18}-Cbl-DEX-loaded erythrocytes do not release their therapeutic contents (Figure S12, S14, and S16 (SI)).

We also examined whether C_{18}-Cbl-drug conjugates transfer from erythrocytes to HeLa cells in the absence of light. HeLa cells were incubated with C_{18}-Cbl-DEX-loaded erythrocytes and, subsequently, the adherent HeLa cells were washed to remove the red blood cells. If C_{18}-Cbl-DEX had migrated to HeLa membranes during the incubation process, illumination at 525 nm should result in DEX release, uptake, and GRα migration. However, we did not observe receptor relocation to the nucleus, suggesting that C_{18}-Cbl-DEX is retained by erythrocytes in the dark (Figure S17 (SI)).

With the biological efficacy of the light-triggered release of drugs from erythrocytes established, we turned our attention to the assembly of photoresponsive constructs that 1) operate within the optical window of tissue and 2) are encoded to respond to specific wavelengths. Our choice of anti-inflammatory drugs is based upon their role in the treatment of rheumatoid arthritis (RA). The long-term administration of anti-inflammatory agents produces moderate to severe side effects, such as weight gain, osteoporosis, diabetes mellitus, hypertension, skin fragility, and infections arising from the systemic immunocompromised state.[13,14] Not surprisingly, there is significant interest in the development of therapeutics that can be selectively delivered to RA joints.[15] With this in mind, we prepared C_{18} derivatives of Cy5 (C_{18}-Cy5; $\lambda_{ex} = 646$ nm), AlexaFluor 700 (C_{18}-AF700; $\lambda_{ex} = 700$ nm), Cy7 (C_{18}-Cy7; $\lambda_{ex} = 747$ nm), and a DyLight 800 analogue (C_{18}-DY800; $\lambda_{ex} = 784$ nm) and examined whether they are capable of serving as long-wavelength antennas for drug release. Photolysis experiments employed in-house-constructed LED circuit boards centered at 660 nm (Cy5), 725 nm (AF700 and Cy7), and 780 nm (DY800) (Figure S18 and Table S7 (SI)).

Our initial studies employed C_{18}-Cbl-TAM in the presence of the C_{18}-fluorophores, since the photorelease of TAM from C_{18}-Cbl-TAM-labeled erythrocytes is readily monitored by fluorescence. In order to identify optimal energy transfer conditions, we first exposed erythrocytes to various relative concentrations of C_{18}-Cbl-TAM and C_{18}-Cy5. After the erythrocytes had been washed to remove any unbound C_{18}-Cbl-TAM and C_{18}-Cy5, the loaded red blood cells were illuminated at 660 nm. The carrier erythrocytes were subsequently pelleted by centrifugation and TAM fluorescence in the supernatant was measured. Although the most efficient TAM release was observed with erythrocytes exposed to a 1 μM:10 μM ratio of C_{18}-Cbl-TAM:C_{18}-Cy5 (Figure S19 (SI)), we employed a 1 μM:5 μM ratio to keep disruption of the erythrocyte's structural integrity at an absolute minimum. In addition to the C_{18}-Cy5 @ 660 nm antenna, the photorelease of TAM from C_{18}-Cbl-TAM-loaded erythrocytes can be triggered at longer wavelengths in the presence of other antennas [C_{18}-Cy7 @ 725 nm, C_{18}-Cy7 @ 725 nm, C_{18}-DY800 @ 780 nm]. Figure 4 compares the fraction of TAM released as a function of antenna wavelength, power of the different LEDs, and photon density. An analogous set of experiments with similar results was performed with C_{18}-Cbl-FAM/C_{18}-fluorophores (Figure S20 (SI)). Erythrocytes in the dark do not release TAM or FAM and, erythrocytes lacking a fluorophore antenna do not release FAM or TAM at wavelengths longer than those absorbed by Cbl (Figures S21–S23 (SI)). Finally, confocal microscopy revealed that the structural integrity of erythrocytes is not altered by the addition of the C_{18}-fluorophores (Figure S24 (SI)).

We subsequently examined drug photorelease from the erythrocyte-assembled drug/antenna array. C_{18}-Cbl-MTX, C_{18}-Cbl-COL, and C_{18}-Cbl-DEX were each paired with C_{18}-fluorophores and illuminated. LC-MS confirmed the release of MTX, COL, and DEX at the wavelength absorbed by the partner C_{18}-fluorophore (Figures S25 and S26 and Table S8 (SI)):

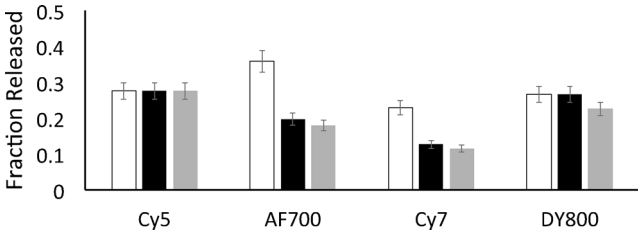

Figure 4. Photorelease of TAM from C_{18}-Cbl-TAM/C_{18}-fluorophore-loaded erythrocytes. LED arrays centered at 660 nm (Cy5), 725 nm (AF700 and Cy7), and 780 nm (DY800) were employed as the light sources. TAM release is displayed as the fraction liberated from erythrocytes. Total erythrocyte-bound C_{18}-Cbl-TAM was determined in a time study where 3 h of illumination generated maximal TAM release. White bars: fraction of TAM release; black bars: fraction of TAM release normalized by the power of the different light sources; gray bars: fraction of TAM release normalized by photon density produced by the light sources; $n = 3$ for all experiments. See the legend to Figure 20 (SI) for an explanation of the normalizations.

C_{18}-Cbl-DEX/C_{18}-Cy5: DEX is released from C_{18}-Cbl-DEX/C_{18}-Cy5-loaded erythrocytes in culture with HeLa cells upon 660 nm illumination. As a consequence, GRα in HeLa cells migrates from the cytoplasm to the nucleus (Figure 5 a,b). By contrast, C_{18}-Cbl-DEX-loaded erythrocytes lacking a long-wavelength-absorbing antenna fail to trigger GRα migration

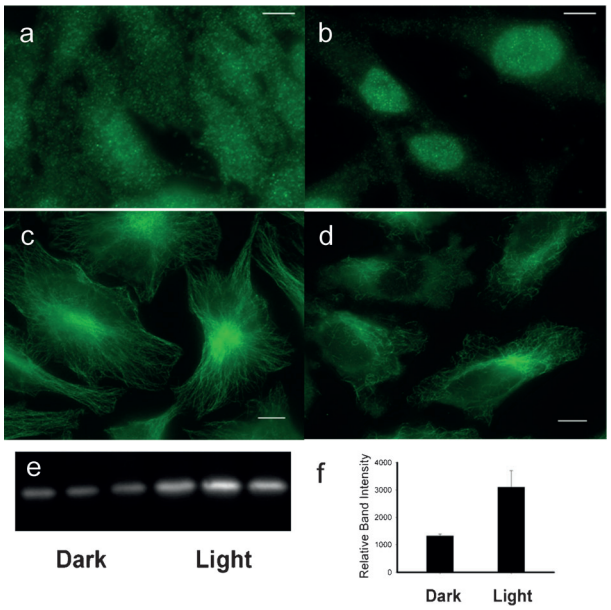

Figure 5. Release of anti-inflammatory agents from erythrocytes and their affect on HeLa cells. a,b) DEX release from C_{18}-Cbl-DEX/C_{18}-Cy5-loaded erythrocytes at 660 nm triggers HeLa cell GRα nuclear localization, where (a) is dark and (b) 660 nm. HeLa GRα visualized with Alexa488 antiRabbit/anti-GRα. c,d) COL release from Cbl-COL/C_{18}-DY800 erythrocytes at 780 nm initiates HeLa microtubule depolymerization, where (c) is dark and (d) 780 nm. HeLa microtubules visualized with Alexa488 antiMouse/anti-tubulin. All scale bars = 5 μm. e,f) MTX release from C_{18}-Cbl-MTX/C_{18}-Cy7-loaded erythrocytes at 725 nm shifts the thermal stability of DHFR where left three lanes (dark) and right three lanes (725 nm). GAPDH used as loading control (Figure S30 (SI)).

when exposed to long wavelengths (e.g. 780 nm; Figures S27 and S28 (SI)).

C_{18}-Cbl-COL/C_{18}-DY800: Irradiation at 780 nm elicits COL release from erythrocyte-anchored C_{18}-Cbl-COL/C_{18}-DY800, which induces microtubule depolymerization in the plated HeLa cells (Figure 5c,d; Figure S29 (SI)).

C_{18}-Cbl-MTX/C_{18}-Cy7: MTX is released from C_{18}-Cbl-MTX/C_{18}-Cy7-loaded erythrocytes upon 725 nm illumination. The MTX photoproduct associates with endogenous DHFR in the cocultured HeLa cells, as assessed by the cellular thermal shift assay (Figure 5e).[16]

In summary, we have described the cell-mediated assembly of photoresponsive drug-release constructs. Release is triggered upon exposure to far-red and near-IR light that falls well within the optical window of tissue. Furthermore, drug release is wavelength-encodable, such that the action wavelength can be chosen in advance based upon the known excitation properties of a given fluorophore. Finally, although this study focused on erythrocytes as drug carriers, the strategy described herein should prove applicable to nanoparticle drug carriers as well.[17]

Received: June 13, 2014
Published online: August 22, 2014

Keywords: cobalamins · drug delivery · photochemistry · prodrugs

[1] J. P. Celli, B. Q. Spring, I. Rizvi, C. L. Evans, K. S. Samkoe, S. Verma, B. W. Pogue, T. Hasan, *Chem. Rev.* **2010**, *110*, 2795 – 2838.

[2] B. J. Tromberg, N. Shah, R. Lanning, A. Cerussi, J. Espinoza, T. Pham, L. Svaasand, J. Butler, *Neoplasia* **2000**, *2*, 26 – 40.

[3] a) H. M. Lee, D. R. Larson, D. S. Lawrence, *ACS Chem. Biol.* **2009**, *4*, 409 – 427; b) P. Klan, T. Solomek, C. G. Bochet, A. Blanc, R. Givens, M. Rubina, V. Popik, A. Kostikov, J. Wirz, *Chem. Rev.* **2013**, *113*, 119 – 191.

[4] G. Bort, T. Gallavardin, D. Ogden, P. I. Dalko, *Angew. Chem.* **2013**, *125*, 4622 – 4634; *Angew. Chem. Int. Ed.* **2013**, *52*, 4526 – 4537.

[5] G. Chen, H. Qiu, P. N. Prasad, X. Chen, *Chem. Rev.* **2014**, *114*, 1236 – 1250.

[6] T. A. Shell, J. R. Shell, Z. L. Rodgers, D. S. Lawrence, *Angew. Chem.* **2014**, *126*, 894 – 897; *Angew. Chem. Int. Ed.* **2014**, *53*, 875 – 878.

[7] V. R. Muzykantov, *Expert Opin. Drug Delivery* **2010**, *7*, 403 – 427.

[8] a) D. Dolphin, A. W. Johnson, R. Rodrigo, *Ann. N. Y. Acad. Sci.* **1964**, *112*, 590 – 600; b) R. T. Taylor, L. Smucker, M. L. Hanna, J. Gill, *Arch. Biochem. Biophys.* **1973**, *156*, 521 – 533; c) J. Halpern, S.-H. Kim, T. W. Leung, *J. Am. Chem. Soc.* **1984**, *106*, 8317 – 8319; d) P. M. Kozlowski, M. Kumar, P. Piecuch, W. Li, N. P. Bauman, J. A. Hansen, P. Lodowski, M. Jaworska, *J. Chem. Theory Comput.* **2012**, *8*, 1870 – 1894.

[9] M. A. Priestman, T. A. Shell, L. Sun, H. M. Lee, D. S. Lawrence, *Angew. Chem.* **2012**, *124*, 7804 – 7807; *Angew. Chem. Int. Ed.* **2012**, *51*, 7684 – 7687.

[10] a) J. J. McGuire, *Curr. Pharm. Des.* **2003**, *9*, 2593 – 2613; b) D. J. Antonjuk, D. K. Boadle, H. T. A. Cheung, M. L. Friedlander, P. M. Gregory, M. H. N. Tattersall, *Arzneim.-Forsch.* **1989**, *39*, 12 – 15.

[11] a) B. D. Markovic, S. M. Vladimirov, O. A. Cudina, J. V. Odovic, K. D. Karljikovic-Rajic, *Molecules* **2012**, *17*, 480 – 491; b) C. Civiale, F. Bucaria, S. Piazza, O. Peri, F. Miano, V. Enea, *J. Ocul. Pharmacol. Ther.* **2004**, *20*, 75 – 84.

[12] D. Richter, P. G. Croft, *Biochem. J.* **1942**, *36*, 746 – 757.

[13] D. Huscher, K. Thiele, E. Gromnica-Ihle, G. Hein, W. Demary, R. Dreher, A. Zink, F. Buttgereit, *Ann. Rheum. Dis.* **2009**, *68*, 1119 – 1124.

[14] U. Baschant, N. E. Lane, J. Tuckermann, *Nat. Rev. Rheumatol.* **2012**, *8*, 645 – 655.

[15] a) S. Mitragotri, J. W. Yoo, *Arch. Pharmacal Res.* **2011**, *34*, 1887 – 1897; b) C. Fiehn, *Clin. Exp. Rheumatol.* **2010**, *28*, S40 – 45; c) W. Ulbrich, A. Lamprecht, *J. R. Soc. Interface* **2010**, *7* Suppl 1, S55 – 66.

[16] D. M. Molina, R. Jafari, M. Ignatushchenko, T. Seki, E. A. Larsson, C. Dan, L. Sreekumar, Y. Cao, P. Nordlund, *Science* **2013**, *341*, 84 – 87.

[17] a) A. Puri, *Pharmaceutics* **2013**, *6*, 1 – 25; b) R. Tong, D. S. Kohane, *Wiley Interdiscip. Rev. Nanomed. Nanobiotechnol.* **2012**, *4*, 638 – 662; c) C. Alvarez-Lorenzo, L. Bromberg, A. Concheiro, *Photochem. Photobiol.* **2009**, *85*, 848 – 860.

